Semicond. Sci. Technol. **22** (2007) 663–670 doi:10.1088/0268-1242/22/6/014

Influence of the surface charge on the operation of ballistic T-branch junctions: a self-consistent model for Monte Carlo simulations

I Iñiguez-de-la-Torre[1], J Mateos[1], T González[1], D Pardo[1], J S Galloo[2], S Bollaert[2], Y Roelens[2] and A Cappy[2]

[1] Departamento de Física Aplicada, Universidad de Salamanca, Plaza de la Merced s/n, 37008 Salamanca, Spain
[2] Institut d'Electronique de Microélectronique et de Nanotechnologie (IEMN), Département Hyperfréquences et Semiconducteurs, BP 69, 59652 Villeneuve d'Ascq Cédex, France

E-mail: indy@usal.es

Received 16 March 2007, in final form 19 April 2007
Published 21 May 2007
Online at stacks.iop.org/SST/22/663

Abstract
We analyse the influence of the surface charge on the operation of ballistic T-branch junctions by means of a semi-classical 2D Monte Carlo simulator. We propose a new self-consistent model in which the local value of the surface charge is dynamically adjusted depending on the surrounding carrier density. The well-known parabolic behaviour of the central branch potential V_C when biasing right and left branches in a push–pull fashion is found to be much influenced by the value of the surface charge in both the horizontal and vertical branches. With the help of experimental measurements performed in real devices, the influence of the width of the central branch on the values of V_C and its relation to surface charge effects are also studied.

(Some figures in this article are in colour only in the electronic version)

1. Introduction

Great efforts have been made in recent years to fabricate new nanometre-sized electronic devices [1–5]. At this scale most of the studies have focused on electron transport properties, while less attention has been paid to surface effects in these nanostructures. As the size of electronic devices is reduced, the surface–volume ratio increases considerably and, in strong contrast to conventional devices, when dimensions reach the nanometric scale, surface effects can get to have a remarkable importance on electron transport, even becoming decisive in the device behaviour [6–8].

As is well known, the origin of surface charge in dielectric/semiconductor interfaces is the rupture of the crystal periodic potential. As a consequence, new states localized at the semiconductor surface with energies within the gap appear and can be occupied by electrons. Recently proposed devices, called self-switching diodes, base their operation on these surface sidewall charges [6]. Monte Carlo (MC) simulations [9] are able to explain the physics of these devices by simply modelling the surface states through a constant negative surface charge density σ placed at the semiconductor–air interfaces [8]. However, some features of these surface charges make it difficult to implement them precisely in a MC simulator. The occupation of the surface states depends not only on the energy level, but also on the potential profile and the Fermi energy in the surrounding region (these aspects are the basis of a recently proposed new concept of a nanoscaled memory point, the self-switching memory [7]). Moreover, surface physical and chemical properties, fabrication processes, surface oxidation, composition and roughness determine the properties of the surface states and, as a consequence, the response of nanometre-scale devices. In addition, the capture and emission mean times of surface states (with values typically in the μs range) are much higher than scattering times,

thus preventing their detailed treatment in a microscopic MC scheme, since a huge CPU time would be necessary to take into account the correct dynamics of these states. Another possibility in obtaining a stationary profile of the surface charge is to solve the trap occupancy and the MC carrier concentration iteratively. However, for this the properties of the traps (density, cross-section and energy distribution) must be known, which is not our case. In this context, the aim of the present paper is to develop a new model, based on the depletion induced by traps and not on their statistics, in which the local value of the surface charge is updated self-consistently with the carrier dynamics near the interface during the simulation. This model completes and improves previous works [10–12] where a constant surface charge density (neither depending on the position nor on the applied potential [13, 14]) was considered at the semiconductor–dielectric interfaces associated with the presence of surface states. The new model will be applied to investigate the influence of the surface charges on the output voltage V_C measured at the bottom of the (open circuited) vertical branch of T-shape three-terminal ballistic junctions (TBJs) fabricated with different widths of the vertical branch W_{VER}.

Previous works [4, 12, 15] show that when electron transport is ballistic and TBJs are biased in a push–pull fashion, V_C is found to be always negative (as long as $V \neq 0$), whereas if transport is diffusive one would simply expect $V_C = 0$ regardless of the input potential. The basic operation of TBJs has been explained in terms of space-charge effects originating from the joint action of surface charges at the semiconductor–air interfaces and inhomogeneous charge distributions associated with the ballistic motion of carriers along the channel [12, 16]. Simulations [12] and experiments [4, 15] showed that V_C is a quadratic function of V for small applied potentials, as predicted in [17]. In this work we will show how a reduction in the width of the vertical branch leads, by means of the influence of the surface charges, to more negative values of the central branch potential, as observed in experiments.

The outline of the paper is as follows. In section 2 we explain the physical model used for the simulation of ballistic structures, with a special emphasis on the treatment of surface charge. In section 3, details about the fabrication and topology of the structures will be given. In section 4, which shows the main results, the validity of our approach will be checked by a comparison of the simulations with experimental measurements. With the aid of the microscopic description provided by the MC simulator, the influence of the surface charges and the size of the branches on the bottom output voltage V_C will be explained in terms of the simulated surface charge, potential and carrier concentration profiles. Finally, section 5 summarizes the main conclusions and future perspectives of the present work.

2. Physical model

2.1. Monte Carlo model

For the correct modelling of real devices, a 3D simulation would be necessary in order to take into account the effect of the lateral surface charges and the real topology of the structures. For simplicity we make use of a semi-classical ensemble MC simulator self-consistently coupled with a 2D Poisson solver [18, 19], where some assumptions, described in [11, 12], are made. The real layer structure of the devices is not included in the (top-view) simulations and only the $In_{0.70}Ga_{0.30}As$ channel is considered. To account for the fixed positive charges of the whole layer structure, a net background doping $N_{db} = 10^{17}$ cm^{-3} is assigned to the channel when solving the Poisson equation, but impurity scattering is switched off; in this way, electron transport through the undoped channel is well described. On the other hand, a negative surface charge density σ is assigned to the semiconductor–air interfaces to account for the influence of the surface states (figure 1(*b*)). The non-simulated dimension Z (used for the comparison of the simulated values of current with those measured in real devices) was estimated as $Z = n_s/N_{db} = 2 \times 10^{-5}$ cm, with $n_s = 2 \times 10^{12}$ cm^{-2}, a typical value of sheet electron density in the fabricated InGaAs channels. We remark that the results of the simulations for V_C (figure 1(*b*)) have been obtained by subtracting the equilibrium value of the electrostatic potential to allow for the comparison with experimental measurements.

2.2. Self-consistent surface charge model

Sidewall surface charge provokes the depletion of part of the conducting channel as a consequence of Coulomb repulsion and thus lowers the carrier density near the interface with the dielectric. In the total depletion approximation, the depletion width originated by a surface charge σ is $W_d = \sigma/N_{db}$ at each side of the channel. Therefore, the effective conduction width is $W_{eff} = W - 2W_d$, with W being the total width of the channel. With the aim of extracting the experimental lateral depletion width W_d, the electrical characterization of channels with different length and width has been done. A value of W_d about 40 nm (±10 nm) for $In_{0.7}Ga_{0.3}As$ channels [20], corresponding to a surface charge density of $\sigma/q = (0.4 \pm 0.1) \times 10^{12}$ cm^{-2} (using $N_{db} = 10^{17}$ cm^{-3}), has been obtained near equilibrium conditions.

A simple way to include the influence of this surface charge in MC simulations is to consider a simple model in which σ is fixed to the experimentally extracted equilibrium value, and kept constant independently of the topology of the structure, position along the interface, bias and time. This model will be denoted as a constant charge model (CCM). The surface charge is included as a Neumann boundary condition for the Poisson equation: $\varepsilon_2 E_2^n - \varepsilon_1 E_1^n = \sigma$, with ϵ_i the permittivity and E_i^n the normal electric field in the ith material. However, the use of this model cannot be justified for W lower than 80 nm (W_{eff} becomes negative) since when the channel is totally depleted, the surface states should not be susceptible to be occupied by free electrons and σ should decrease. In such a case ($W_{eff} < 0$), if the CCM is used, the background doping N_{db} cannot compensate the negative surface charge, charge neutrality is not ensured and unphysically high negative potentials are obtained in the simulation, providing incorrect results. To solve these problems, we propose an *ad hoc* self-consistent charge model (SCCM) able to reproduce more closely the surface charge effects.

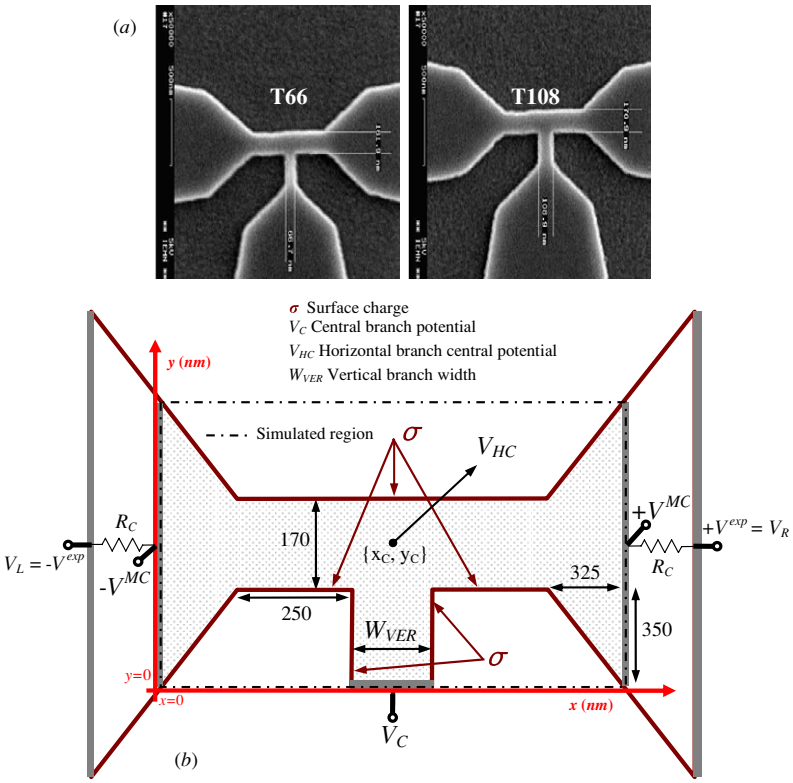

Figure 1. (*a*) SEM images of the TBJs with 66 and 108 nm wide vertical branches. They will be denoted as T66 and T108, respectively. (*b*) Schematic representation of the simulated T-branch junctions. Dimensions of the accesses, horizontal and vertical branches are indicated in nm.

The philosophy of our new self-consistent model is based on the adaptation of the value of the surface charge to the carrier density in the nearby region. First, we evaluate the carrier concentration next to the boundary (N_{front}) as an average over a given number of iterations N_i. Then, it is checked if N_{front} has a value in the range (N_{low}, N_{high}) with $N_{\text{low}} = N_{\text{db}}/\text{Fact}_{\text{low}}$ and $N_{\text{high}} = N_{\text{db}}/\text{Fact}_{\text{high}}$, which represent the limits to which we try to adapt the electron concentration next to the interface. If the concentration (N_{front}) is higher than the upper limit (N_{high}), we increase the surface charge by a given amount $\Delta\sigma$, so that its repulsive effect provokes stronger channel depletion and thus the concentration should diminish. On the other hand, if N_{front} is smaller than the lower limit (N_{low}), the surface charge is decreased by the same density $\Delta\sigma$ to reduce the (too large) induced depletion. The choice of the limits N_{low}, N_{high} is constrained by the level of statistical resolution achievable by the simulation (which depends on the number of simulated electrons). If the lower limit is too low (the forced depletion level is too strong), below the value of electron concentration that MC simulations can reliably estimate, wrong results would be obtained. Additionally, two counters ($\text{Times}_{\text{increase}}$, $\text{Times}_{\text{decrease}}$) have been introduced to control the increase/decrease of the surface charge, so that the condition to change σ must be verified a certain number of times (given by the respective counters) for the modification to take place.

An optimization of the values of the parameters to improve the efficiency of the algorithm and the agreement with experimental results has been made. The selected values are $\text{Fact}_{\text{high}} = 50$, $\text{Fact}_{\text{low}} = 100$, $\text{Times}_{\text{increase}} = 1$, $\text{Times}_{\text{decrease}} = 5$ and $\Delta\sigma = 10^{-10}\,\text{cm}^{-2}$. Every $N_i = 500$ iterations, the value of N_{front} is recalculated and the surface charge update algorithm is carried out. N_i has been chosen as a trade-off to optimize the precision of the time-dependent electron concentration without much increasing the run-time of the simulation. Neither N_i nor $\Delta\sigma$ significantly influence the final results, though they can eventually modify the time it takes to reach the stationary surface charge profiles.

To conclude, it is important to remark that evidently this *ad hoc* surface charge model is not able to reproduce the statistics of occupation of surface states, but it does describe correctly the global effect of the surface charge. We will apply this self-consistent model to study T-shaped TBJs based on InAlAs/InGaAs layers and compare the results with experimental measurements, achieving a satisfactory agreement.

3. Fabricated and simulated devices

The fabrication process and experimental characterization have been carried out in the Institut d'Electronique, de Microélectronique et de Nanotechnologie du Nord (IEMN), Villeneuve d'Ascq, France. The layer structure, grown by molecular beam epitaxy (MBE), consists of an InP substrate, a 200 nm $Al_{0.48}In_{0.52}As$ buffer followed by a 15 nm $In_{0.70}Ga_{0.30}As$ strained channel, three layers of $Al_{0.48}In_{0.52}As$ (a 5 nm spacer, a δ-doped layer and a 10 nm Schottky layer) and, finally, a 15 nm $In_{0.53}Ga_{0.47}As$ cap layer. The geometry of the TBJs was defined by a high resolution negative e-beam resist, Hydrogen Silses Quioxane (HSQ), exposed by

a LEICA EBPG5000 + machine, and $CH_4/H_2/Ar$ reactive ion etching (RIE) [20]. Then Ni–Ge–Au–Ni–Au metals were evaporated and annealed to form ohmic contacts and, finally, Ti–Au bonding pads were realized.

In principle, RIE is more aggressive than wet etching and could produce serious damage to the sidewalls. However, we have fabricated structures with both techniques, and similar values of the depletion depth (40 ± 10 nm) were obtained, as reported in [20]. Moreover, within our fabrication process for these extremely small devices, the undercut and roughness generated by RIE are much smaller than those produced by wet etching. That is why we adopted RIE as the etching technique for our ballistic devices.

Five TBJs with different widths of the vertical branch, W_{VER} = 66, 78, 84, 94 and 108 nm, have been fabricated. Scanning electron microscope (SEM) images of the TBJs with 66 and 108 nm wide vertical branches are shown in figure 1(*a*). For our MC analysis, we consider the geometry shown in figure 1(*b*). It consists of a non-uniform mesh of 86 × 48 cells. The dimensions of the branches (identical to the experimental ones) and the coordinate system are indicated in the figure. The voltage V_C is calculated by averaging the electric potential (and subtracting the equilibrium value) at the bottom of the (open circuited) central branch. We will also show results for the value of the electric potential at the centre of the horizontal channel, which will be denoted as V_{HC}. As concerns the accesses, we have checked that for correct modelling it is enough to include a part of the access region in the simulated domain, and then add a series resistance R_C to account for the potential drop in the non-simulated portion of the accesses (of the order of 300 nm) [3]. The value of the series resistance used in the MC calculations is $R_C = 1.3 \times 10^{-4}$ Ω m, which implies R_C = 650 Ω (for a non-simulated dimension $Z = 2 \times 10^{-7}$ m). Thus, to compare with an experimental applied voltage V^{exp}, the value considered in the MC simulation is $V^{MC} = V^{exp} - R_C \times I$, where I is the current flowing through the horizontal branches (see figure 1).

4. Results

Figure 2(*a*) shows the experimental values of the potential V_C in the central branch (measured with a high-impedance voltmeter) and the current I flowing through the horizontal branches in the TBJs when biased in a push–pull fashion ($V_R = +V$ and $V_L = -V$ applied to the right and left branches, respectively). The parabolic behaviour of V_C is strengthened when reducing the width of the vertical branch, which means that T66 generates higher (negative) values of V_C. This is in principle an unexpected result, since the vertical branch is believed to be only a measure (passive) element [11, 12], in such a manner that the value of V_C should be independent of its width W_{VER}. The inset of figure 2(*a*) shows how, as expected, the current is independent of W_{VER}, since the horizontal branch is practically identical for the different TBJs.

We have tried to reproduce these measurements with MC simulations using the CCM for the surface charge with $\sigma/q = (0.4 \pm 0.1) \times 10^{12}$ cm^{-2} ($W_d \approx 40$ nm), the results being totally inconsistent with experiments. For example, the negative values of the V_C versus V curve reach a maximum for a width of 84 nm, just when the width of the channel nearly coincides

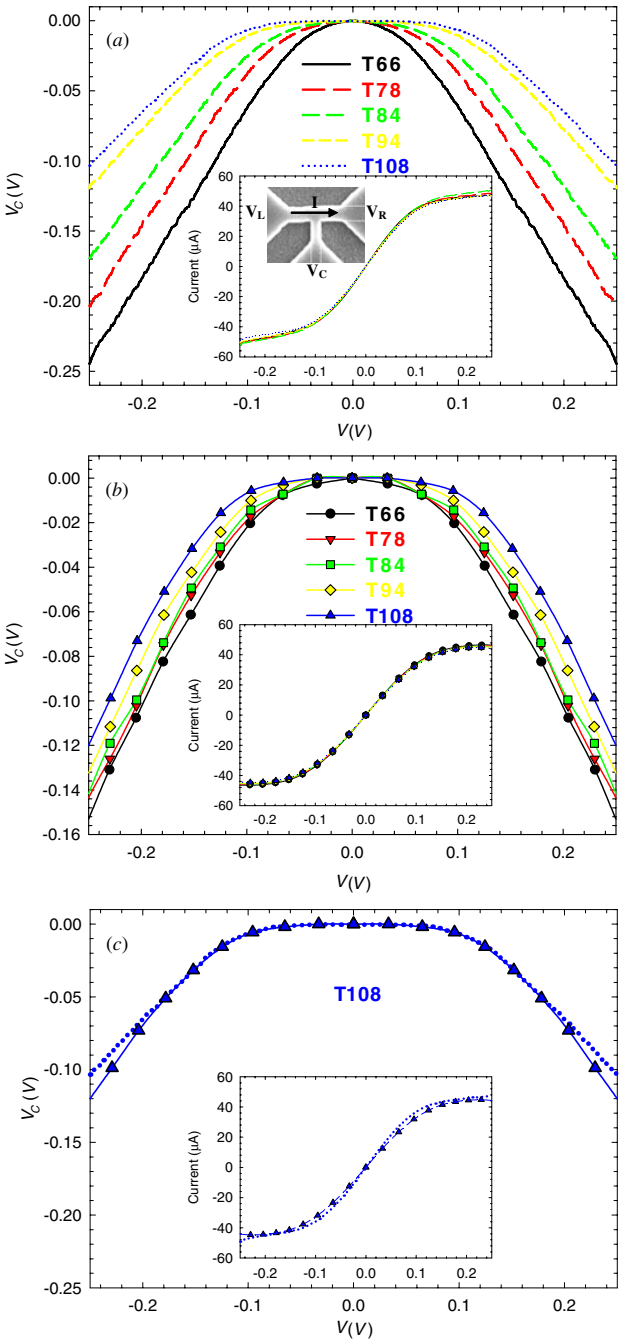

Figure 2. (*a*) Experimental and (*b*) MC values of the bottom potential V_C and current (insets) in the TBJ junctions with 66, 78, 84, 94 and 108 nm wide vertical branches (denoted as T66, T78, T84, T94 and T108, respectively) as a function of the push–pull bias V. (*c*) Comparison of the measured (lines) and simulated (symbols) V_C–V and I–V (inset) characteristics for the T108 junction.

with the lateral depletion induced by the surface charge ($W_{eff} = W - 2W_d \approx 0$). On the other hand, by using a different value of σ, a good fitting could be obtained for one or two of the structures, but not for all of them. Note that the results published (by some of the authors) in [11, 12] for TBJs with a different constant surface charge have the same problem, being incorrect for the highest values of σ (when the branches are completely depleted).

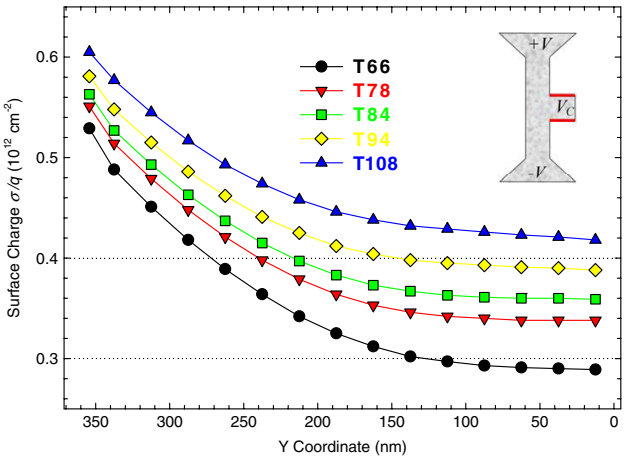

Figure 3. Surface charges in the sidewalls of the vertical branch under equilibrium conditions ($V = 0$).

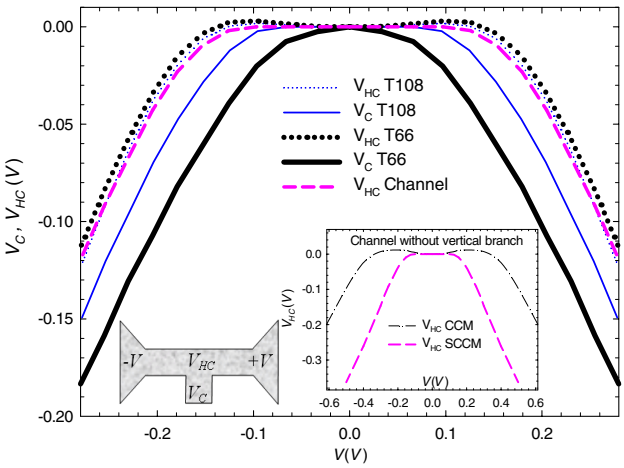

Figure 4. V_{HC} and V_C as a function of the applied voltage for the TBJs with $W_{VER} = 66$ and 108 nm. V_{HC} for a channel without the vertical branch is also plotted for comparison. The inset shows V_{HC} calculated in the channel without the vertical branch with the CCM ($\sigma/q = 0.4 \times 10^{12}$ cm^{-2}) and SCCM models of surface charge.

In contrast, the calculations of V_C shown in figure 2(*b*), performed with the SCCM, are consistent with the experimental results, showing the same trend and satisfactory quantitative agreement. The agreement is excellent for the TBJs with the wider vertical branches (T94 and T108). Figure 2(*c*) shows the comparison of simulated and measured values of V_C and I for the particular case of T108, with outstanding agreement. When W_{VER} is decreased, the simulated $V_C - V$ curves, while following the same trend as measurements (higher negative values for lower W_{VER}, with a quadratic shape at low bias), do not increase their parabolicity as much as in experiments. Finally, concerning the current (insets of figures 2(*b*) and (*c*)), the agreement is totally satisfactory for the whole set of junctions, both qualitatively and quantitatively. Let us try to understand the previous results by means of the information provided by MC simulations.

Firstly, we remark that the proposed SCCM allows for the variation of the surface charge σ along the position in the interface in accordance with the surrounding free carrier concentration. Figure 3 shows the profiles of surface charge along the vertical branch in the five junctions obtained under equilibrium conditions ($V = 0$). This possibility of self-adaptation allows the surface charge in the narrowest junction (T66) to reach values that approximately cause a total depletion of the vertical branch, $\sigma/q = 0.3 \times 10^{12}$ cm^{-2}. In contrast, in the widest junction (T108) the surface charge is limited by a value close to that obtained in the experimental measurements, $\sigma/q = (0.4 \pm 0.1) \times 10^{12}$ cm^{-2} [20]. These facts support the physical consistency of our model. Furthermore, the surface charges take a value practically constant near the bottom of the vertical branch, which indicates that the results will not change if this branch is made longer.

Surface charges are very important for the operation of the TBJs, since, as we will show, the values of V_C depend on the amount of charge present in the vertical branch and its evolution with the bias. In the following, we will analyse the microscopic results provided by the MC simulator concerning not only the values of the surface charges but also their influence on the carrier concentration and electric potential profiles, both along the horizontal and vertical branches. We will focus on the structures with the widest (T108) and the narrowest (T66) central branches. Three different biasing values ($V = 0$, 0.125 and 0.25 V) will be typically considered, trying to provide an explanation for the increase of the negative values of V_C as the width of the vertical branch is reduced.

In previous works (using the CCM for the surface charges) [11, 12] the vertical branch was considered as a voltage probe, providing at its bottom (V_C) the variations of V_{HC} (potential at the centre of the horizontal branch). However, within the SCCM, the surface charge in the sidewalls of the vertical branch and the carrier penetration inside it change with the bias (as in Y-junctions [12]), which means that V_C is no longer a faithful reflection of the V_{HC} variations. It is thus necessary to consider the electric potential difference ΔV_V between V_C and V_{HC}, given by the electric field circulation $\Delta V_V = -\int_{y=0}^{y=y_C} \bar{E} \cdot d\bar{l}$ throughout the vertical branch, which obviously will not be equal for all the applied voltages. Therefore, the values of V_C can be considered as the result of two combined effects: a horizontal one (given by the variation of V_{HC} with the bias) and a vertical one (given by the variation of ΔV_V with the bias).

We analyse first the difference between V_{HC} and V_C. In figure 4, we plot the values obtained with the MC simulations for V_{HC} in T66 and T108, together with those calculated in a channel without the vertical branch. It can be observed that the values of V_{HC} practically coincide in the three structures. Bearing in mind that transport takes place in the horizontal direction and the width and length of the horizontal branch are practically the same in the three cases, the evolution of V_{HC} with V is expected to be analogous. In fact, the concentration and electrostatic potential profiles along the horizontal branch are very similar in the two TBJs, as can be observed in figure 5. In this figure, the perturbation caused by the vertical branch in the horizontal profiles of both concentration and potential is evidenced (displaying even a hump). The absence of surface charges at the bottom interface due to the presence of the vertical branch leads to a less important depletion (and thus to a higher electron concentration) in the centre of the horizontal

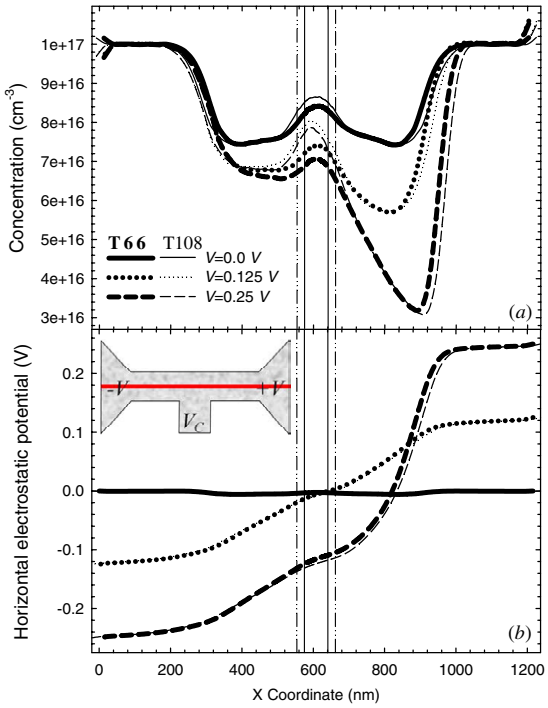

Figure 5. Profiles of (*a*) carrier concentration and (*b*) electrostatic potential along the centre of the horizontal branch of the TBJs with $W_{VER} = 66$ nm (thick lines) and 108 nm (thin lines) for $V = V_R = -V_L = 0.0$, 0.125 and 0.25 *V*.

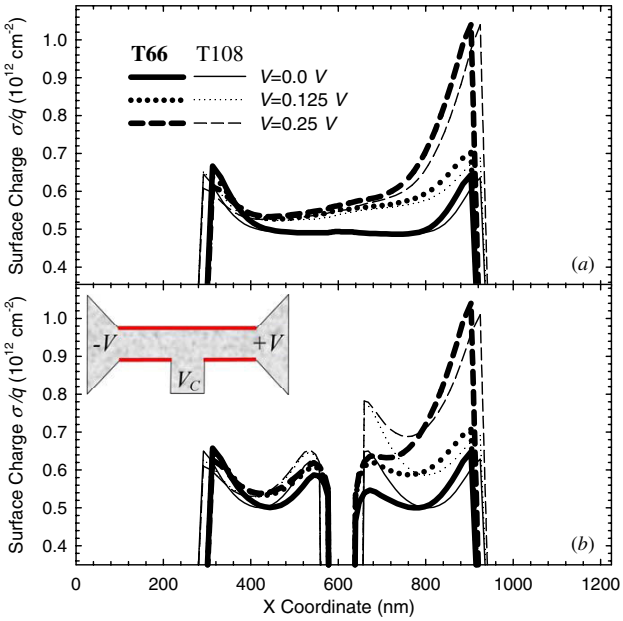

Figure 6. Surface charge profiles in (*a*) the top and (*b*) the bottom boundaries of the horizontal branch of T66 and T108 for $V = 0.0$, 0.125 and 0.25 V.

branch. In figure 5, it is also observed that for T108 this effect is stronger than for the narrower T66, mainly in the concentration; indeed the potential profiles are only slightly modified by the presence of the vertical branch (or its width). As a consequence, the values of V_{HC} hardly depend on the width of the central branch, and even on the presence or absence of this branch, as observed in figure 4.

The inset of figure 4 compares the values of V_{HC} in a simple channel (without the vertical branch) obtained with the CCM and SCCM models of surface charge. The SCCM leads to a considerable increase in the negative values of V_{HC}, which is the signature of an enhanced charge asymmetry in the horizontal direction. Such an asymmetry can be observed in figure 5 for high values of V, for which a strong depletion of carriers takes place at the right part of the horizontal branch. This region becomes highly resistive, so that most of the applied potential drops here and leads to the high negative values of V_{HC}. The presence of ballistic transport in the horizontal direction produces the same qualitative effect (see [11, 12, 16]), but weaker than that observed here, thus originating smaller negative values of V_{HC}, like those obtained with the CCM (inset of figure 4).

This interesting phenomenon, the strong carrier depletion near the anode taking place for high V, is caused by the high surface charge present in this zone of the device. This is illustrated in figure 6, where the values of σ at the (top and bottom) boundaries of the horizontal branch are shown. The origin of the increase of the surface charge with the applied voltage near the anode lies in the fact that, due to the ballistic motion of electrons, their longitudinal energy increases significantly as they approach the right contact. Scattering mechanisms, even if there are very few, produce some energy redistribution, and thus make the transversal energy component also increase. In this way electrons are able to approach the boundaries of the TBJ (in spite of the repulsive effect of the surface charge) and contribute to raise the value of σ. As expected, this effect is more important for higher V. Finally, it is interesting to comment that, though the values of surface charge in T108 are higher than in T66 near the junction of the branches (see figure 6(*b*)), in the region near the anode they are similar, and so are the variations with respect to equilibrium conditions, thus providing similar horizontal profiles of concentration and electric potential (as observed in figure 5).

In view of the previous results, we can conclude that the dependence of V_C on the width of the vertical branch W_{VER} is associated with the changes in the vertical profile of the electrostatic potential (ΔV_V) among the different TBJs, since V_{HC}, accounting for the horizontal effects, does not depend on W_{VER}. In order to study this crucial vertical effect, figure 7 shows the concentration and electric potential profiles along the centre of the vertical branch. In figure 7(*b*), the typical parabolic shape of the potential (associated with a depleted region) is observed. However, the electron concentration is perturbed in the proximities of the junction, not showing total depletion due to the presence of the vertical branch. As concerns the equilibrium case, the difference in electron concentration (figure 7(*a*)) leads to a difference in the electric potential. In figure 7 it can be observed that for T66 the electron density at the bottom of the vertical branch ($y = 0$ nm) is 0.6×10^{16} cm^{-3}, that means a Fermi energy of $E_F^{66} = -0.088$ eV, while for T108 the density is higher, 3.3×10^{16} cm^{-3}, corresponding to $E_F^{108} = -0.044$ eV. The difference in the Fermi energy $\Delta E_F \approx 0.04$ eV is just the same as that between the electric potential values at $y = 0$ nm at equilibrium (figure 7(*b*)).

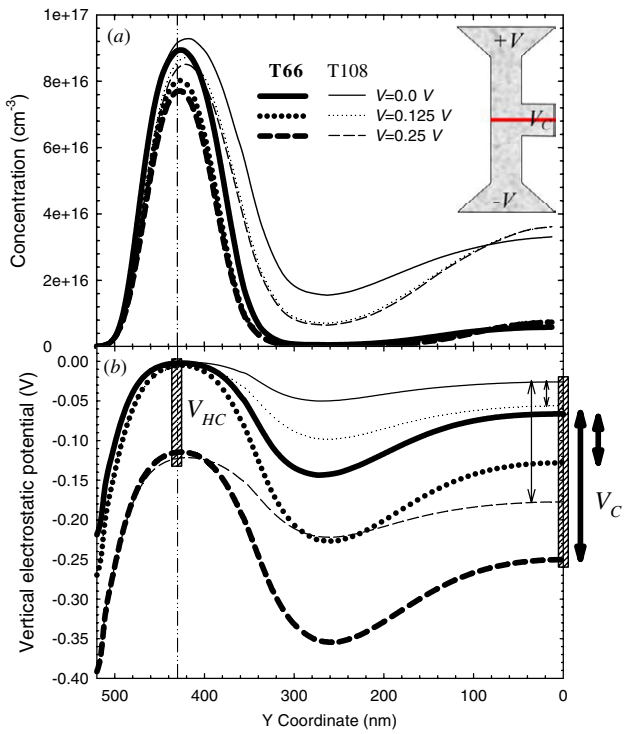

Figure 7. Profiles of (*a*) carrier concentration and (*b*) electrostatic potential along the centre of the vertical branch of T66 (thick lines) and T108 (thin lines) for $V = V_R = -V_L = 0.0$, 0.125 and 0.25 V.

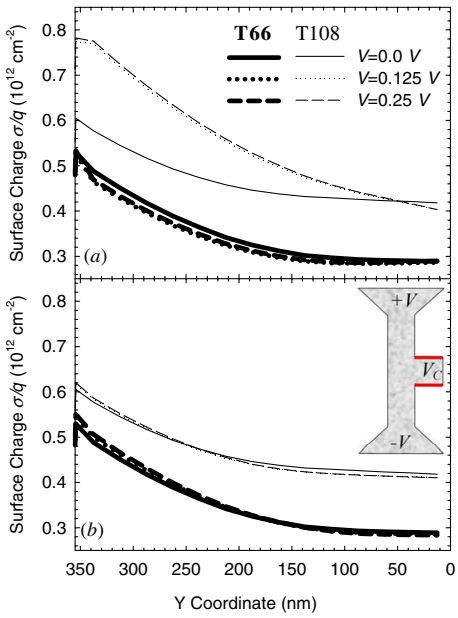

Figure 8. Surface charge profiles in (*a*) the right and (*b*) the left boundaries of the vertical branch of T66 (thick lines) and T108 (thin lines) for $V = 0.0$, 0.125 and 0.25 V.

Regarding the profiles of carrier concentration along the vertical branch as shown in figure 7(*a*), it can be observed that the maximum in the *y*-direction is wider for T108. This means that there is a region in the *y*-direction with a more uniform carrier density, which leads to a smoother variation of the electric potential towards the bottom of the vertical branch, as observed in figure 7(*b*). By means of the Poisson–Helmholtz theorem [21], the electric field could be calculated formally as

$$\mathbf{E}(\mathbf{r}) = -\frac{1}{4\pi\varepsilon}\int_{\infty}\frac{\bar{\nabla}'\rho(\mathbf{r}')}{|\mathbf{r}-\mathbf{r}'|}\mathrm{d}v'$$

Intuitively, this expression indicates that the electric field is intimately related to the inhomogeneities in the carrier density. Thus, the smoother variation of the electron concentration in T108 provides a lower electric field and a smaller potential drop from the centre of the TBJ to the bottom of the vertical branch (figure 7(*b*)).

When the structure is biased, the potential difference with respect to the equilibrium case at the bottom of the central branch, providing the measured electric potential V_C, is higher for T66 than for T108 (figure 7(*b*)). This explains the increasing negative values of V_C versus V obtained as the width of the vertical branch is reduced, figure 2(*b*). As observed in figure 7(*b*), with the SCCM the difference of the electrostatic potentials with respect to the equilibrium case varies along the vertical branch, in contrast with the constant separation (between curves) provided by the CCM [12], where the vertical branch could be considered as a voltage probe not influencing the values of V_C. In fact, the values of V_{HC} are the same in T66 and T108 (approximately zero for $V = 0.125$ V and -0.12 V for $V = 0.25$ V, see figure 4), while those of V_C (potential difference indicated with arrows in the figure) are higher (more negative) in the narrower junction.

In order to explain this effect it is necessary to know not only the free carrier concentration in the vertical branch but also the surface charge profiles in its sidewalls, which are shown in figure 8. As expected, the profiles of σ for $V = 0$ are the same for the right and left boundaries of the vertical branch. Moreover, in the T66 junction the surface charge profile is very similar for all the biasing, since the vertical branch is nearly depleted (figure 7(*a*)). In contrast, in T108 the behaviour of the lateral charges is different: in the right border σ increases with the applied potential, while in the left border it practically does not change. This happens because of the preferential motion of electrons towards the right accelerated by the electric field, thus approaching the right border of the vertical branch. One could expect more negative values of V_C in T108 because of this excess of negative surface charge, but it is not the case, since the variations of σ with respect to equilibrium and the size of the vertical branch also play an important role. Indeed, the proximity of the negative surface charges at the sidewalls of the vertical branch and the possibility for free electrons to enter into this branch are also decisive in the behaviour of V_C. On the other hand, the increase of σ with the bias at the right boundary of the vertical branch in T108 takes place mainly at the top of it, leading to a stronger depletion in this region, while, in contrast, the electron concentration at the bottom even increases with V (figure 7(*a*)), thus raising the value of the electrostatic potential at this point.

In view of the above results, the stronger variation of V_C with V taking place in the TBJs with a narrower vertical branch can be related to the constant carrier concentration in such a branch (which is practically depleted), in contrast with the wider junctions where the variations of the electron concentration at the bottom of the branch compensate the increase of the surface charges at the top of it.

5. Conclusions

The influence of surface charge phenomena on the behaviour of nanometre-scale TBJs has been analysed. We have developed a self-consistent model in which the local value of the surface charge is updated dynamically according to the carrier concentration in the nearby region. The results of the simulations have been favourably compared with the experimental measurements of devices fabricated at the IEMN. This new model provides a good qualitative description of the operation of TBJs with different widths W_{VER} of the vertical branch, providing higher negative values for V_C as W_{VER} is decreased. Moreover, the current flowing through the structures has also been reproduced in a totally satisfactory way.

A strong increase of the depletion near the anode of the TBJs is obtained with the self-consistent surface charge model (due to the increase of energy related to quasiballistic electron transport), thus enhancing the asymmetry of the electron concentration. As a consequence, the values of the potential at the centre of the horizontal branch V_{HC} calculated with this model are significantly higher than those obtained with the CCM.

We have found that V_{HC} is nearly independent of the width of the vertical branch and even of the presence or absence of this branch. Therefore, the dependence of V_C on W_{VER} comes from a vertical effect originating from microscopic processes taking place inside the vertical branch. Due to the bias dependence of the surface charge and electron concentration within this branch, the variations of V_{HC} are not transmitted in the same way to the bottom of the vertical branch when its width is modified. Indeed, an increasing negative value of V_C is found when reducing W_{VER} due to the total depletion of this branch. One could take advantage of this effect to improve the sensitivity or the output power in practical applications of the TBJ, such as power detection or frequency doubling (associated with the characteristic quadratic dependence of the output voltage on the bias, $V_C = -\alpha V^2$). Further studies on the influence of the size (length and width) of the horizontal branch will be performed in order to get a better response of TBJs for such applications.

Acknowledgments

This work has been partially supported by the Dirección General de Investigación (MEC, Spain) and FEDER through the project TEC2004-05231 and by the Consejería de Educación of the Junta de Castilla y León (Spain) through the project SA044A05.

References

[1] Song A M, Lorke A, Kriele A and Kotthaus J P 1998 Nonlinear electron transport in an asymmetric microjunction: a ballistic rectifier *Phys. Rev. Lett.* **80** 3831

[2] Song A M, Omling P, Samuelson L, Seifert W, Shorubalko I and Zirath H 2001 Operation of InGaAs/InP-based ballistic rectifiers at room temperature and frequencies up to 50 GHz *Japan. J. Appl. Phys.* **40** L909

[3] Mateos J, Vasallo B G, Pardo D, González T, Pichonat E, Galloo J S, Bollaert S, Roelens Y and Cappy A 2004 Nonlinear effects in T-branch junctions *IEEE Electron Device Lett.* **25** 235

[4] Shorubalko I, Xu H Q, Maximov I, Omling P, Samuelson L and Seifert W 2001 Nonlinear operation of GaInAs/InP-based three-terminal ballistic junctions *Appl. Phys. Lett.* **79** 1384

[5] Worschech L, Xu H Q, Forchel A and Samuelson L 2001 Bias-voltage-induced asymmetry in nanoelectronic Y-branches *Appl. Phys. Lett.* **79** 3287

[6] Song A M, Missous M, Omling P, Peaker A R, Samuelson L and Seifert W 2003 Unidirectional electron flow in a nanometer-scale semiconductor channel: a self-switching device *Appl. Phys. Lett.* **83** 1881

[7] Song A M, Missous M, Omling P, Maximov I, Seifert W and Samuelson L 2005 Nanometer-scale two-terminal semiconductor memory operating at room temperature *Appl. Phys. Lett.* **86** 042106

[8] Mateos J, Vasallo B G, Pardo D and González T 2005 Operation and high-frequency performance of nanoscale unipolar rectifying diodes *Appl. Phys. Lett.* **86** 212103

[9] Jacoboni C and Lugli P 1989 *The Monte Carlo Method for Semiconductor Device Simulation* (New York: Springer)

[10] Mateos J, González T, Pardo D, Tadyszak P, Danneville F and Cappy A 1996 Numerical and experimental analysis of static characteristics and noise in ungated recessed MESFET structures *Solid-State Electron.* **39** 1629

[11] Mateos J, Vasallo B G, Pardo D, González T, Galloo J S, Roelens Y, Bollaert S and Cappy A 2003 Ballistic nanodevices for terahertz data processing: Monte Carlo simulations *Nanotechnology* **14** 117

[12] Mateos J, Vasallo B G, Pardo D, González T, Galloo J S, Bollaert S, Roelens Y and Cappy A 2003 Microscopic modeling of nonlinear transport in ballistic nanodevices *IEEE Trans. Electron Devices* **50** 1897

[13] Moglestue C 1993 *Monte Carlo Simulation of Semiconductor Devices* (London: Chapman and Hall)

[14] Shur M 1987 *GaAs Devices and Circuits* (New York: Plenum)

[15] Xu H Q, Shorubalko I, Maximov I, Seifert W, Omling P and Samuelson L 2002 A novel device principle for nanoelectronics *Mater. Sci. Eng.* C **19** 417

[16] González T, Mateos J, Pardo D, Bulashenko O M and Reggiani L 1998 Microscopic analysis of shot-noise suppression in nondegenerate ballistic transport *Semicond. Sci. Technol.* **13** 714

[17] Xu H Q 2001 Electrical properties of three terminal ballistic junctions *Appl. Phys. Lett.* **78** 2064

[18] Mateos J, González T, Pardo D, Hoel V, Happy H and Cappy A 2000 Improved Monte Carlo algorithm for the simulation of δ-doped AlInAs/GaInAs HEMTs *IEEE Trans. Electron Devices* **47** 250

[19] González T, Mateos J, Pardo D, Varani L and Reggiani L 1999 Injection statistics simulator for dynamic analysis of noise in mesoscopic devices *Semicond. Sci. Technol.* **14** L37

[20] Galloo J S, Pichonat E, Roelens Y, Bollaert S, Wallart X, Cappy A, Mateos J and González T 2004 Transition from ballistic to ohmic transport in T-branch junctions at room temperature in GaInAs/AlInAs heterostructures *Proc. 2004 Int. Conf. Indium Phosphide and Related Materials (IEEE Catalog 04CH37589)* pp 378–81

[21] Jefimenko O D 1989 *Electricity and Magnetism: An Introduction to the Theory of Electric and Magnetic Fields* 2nd edn (Star City: Electret Scientific)